

Magnetoresistance due to Domain Walls in Micron Scale Fe Wires with Stripe Domains

A. D. Kent^a, U. Ruediger^a, J. Yu^a, S. Zhang^a, P. M. Levy^a, Y. Zhong^b, S. S. P. Parkin^c

^a*New York University, Department of Physics, 4 Washington Place, New York, NY 10003*

^b*Physics Department, City College of the City University of New York, NY 10031*

^c*IBM Research Division, Almaden Research Center, San Jose, CA 95120*

(October 17, 1997, accepted for publication January 1998)

Abstract

The magnetoresistance (MR) associated with domain boundaries has been investigated in microfabricated bcc Fe (0.65 to 20 μm linewidth) wires with controlled stripe domains. Domain configurations have been characterized using MFM. MR measurements as a function of field angle, temperature and domain configuration are used to estimate MR contributions due to resistivity anisotropy and domain walls. Evidence is presented that domain boundaries enhance the conductivity in such microstructures over a broad range of temperatures (1.5 K to 80 K).

I. INTRODUCTION

The low field magnetoresistance (MR) of a ferromagnetic metal depends in a detailed and usually complex manner on its magnetic domain structure. An understanding of this interplay between transport and magnetic properties is important to the miniaturization of magnetic devices to nanoscale dimensions, such as those based on giant magnetoresistance (GMR), and to the interpretation of transport results on magnetic nanostructures. For instance, a recent experiment suggests large MR effects due to domain walls can be observed even at room temperature in simple ferromagnet films [1]. The mechanism proposed is analogous to that operative in GMR—the conductance in the presence of domain walls is reduced due a mixing of minority and majority spin channels in the wall [2,3]. Evidently, this might be exploited in novel magnetoelectronic devices and will effect the properties of conventional GMR devices as such devices are scaled down in size (so that walls may occupy an appreciably fraction of the device). Other research has focused on the use of magnetoresistance as a probe of domain wall dynamics at low temperature in nanometer scale Ni wires [4]. Here it appears that domain boundaries enhance the sample conductance. A novel theoretical explanation has been suggested in which domain walls destroy the electron coherence necessary for weak localization [5] at low temperature. This recent research points to the need for experiments over a range of temperatures on microstructures with well characterized and controllable domain patterns to isolate the important contributions to the MR in small samples.

Here we report on the first of such experiments. Fe microstructures with stripe domains arranged perpendicular to the current direction have been realized to study the effect of domain walls on magnetotransport properties. In the following we discuss the fabrication, magnetic characteristics and transport properties of these wires.

II. FABRICATION AND CHARACTERIZATION

The starting point for these experiments are epitaxial (110) oriented bcc Fe thin films. These films have a large in-plane uniaxial magnetocrystalline anisotropy, with the easy axis parallel to the [001] direction. They are grown using an UHV e-beam evaporator on a-axis (11 $\bar{2}$ 0) sapphire substrates. First a 10 nm thick (110) Mo seed layer is deposited at a substrate temperature of 900 K followed by a 100 nm thick layer of Fe at 510 K [6]. X-ray pole figures show that Fe (110) layers grow with their in-plane [1 $\bar{1}$ 1] axis parallel to the [0001] axis of the sapphire substrate. A small ($< 0.05\%$) and anisotropic in-plane strain is also found, consistent with previous x-ray studies of thinner films [6]. The films are then patterned using projection optical lithography to produce micron scale wires (0.65 to 20 μm linewidths) with the wire oriented perpendicular to the magnetic easy axis. Fig. 1 shows the geometry of a 1 μm linewidth transport structure.

The competition between magnetocrystalline, exchange and magnetostatic interactions in the wire results in a pattern of regularly spaced stripe domains. Varying the linewidth changes the ratio of magnetostatic to domain wall energy and hence the domain size. The magnetic domain configuration is also strongly affected by the magnetic history of the samples. Fig. 2 shows MFM images of the domain configuration of a 1.5 μm (Fig. 2 a and b) and 20 μm wire (Fig. 2 c and d) in zero field with a vertically magnetized tip. These images highlight the domain walls and magnetic poles at the wire edges. Before performing these MFM measurements the wires were magnetized to saturation with a magnetic field transverse (Fig. 2 a and c) or longitudinal (Fig. 2 b and d) to the wire axis. For the 1.5 μm wire in the transverse case the average domain width is 1.7 μm and much larger than in the longitudinal case, where the average domain width is 0.4 μm .

In Fig. 3 the domain width is plotted as a function of wire width. In all samples closure domains of a triangular shape are found near the wire edges. White dotted lines in Fig. 2 a) illustrate the approximate domain structure. In order to determine the MR contributions due to resistivity anisotropy the volume fraction of closure domains (with $\mathbf{M} \parallel \mathbf{J}$) must be

estimated. Fig. 3 also shows this fraction (labeled γ) determined from MFM images after magnetic saturation in either the transverse or longitudinal direction.

III. TRANSPORT PROPERTIES

A. Results

MR measurements were performed in a variable temperature high field cryostat with in-situ (low temperature) sample rotation capabilities. The applied field was always in the plane of the thin film, oriented either longitudinal or transverse to the wire axis. The magnetic history of the sample was carefully controlled and low ac current levels were used ($\sim 10 \mu\text{A}$). Fig. 4 shows representative results at 40 K on two samples with distinct domain configurations; Fig. 4 a), b) a $1.5 \mu\text{m}$ wire and Fig. 4 c), d) a $20 \mu\text{m}$ wire. There is structure to the MR in applied fields less than the saturation field, after which the resistivity increases monotonically with field. Fig. 4 also shows that the $1.5 \mu\text{m}$ wire resistivity depends on its magnetic history, being larger after saturation in the transverse geometry.

The MFM images of domain configurations are performed at room temperature. Thus to correlate low temperature MR measurements with domain configurations we warm the sample to room temperature, cycle the magnetic field to establish a known $\mathbf{H} = 0$ magnetic state, and cool. The resistivity at $\mathbf{H} = 0$ and the MR are unchanged for this sample in both longitudinal and transverse measurement geometry [7]. This is strong evidence that the domain structure is not affected by temperature in this range and consistent with SQUID hysteresis loop measurements [8].

B. Interpretation

There are two important sources of low field low temperature MR which must be considered to interpret this transport data. The first has its origins in spin-orbit coupling [9] and is known as anisotropic magnetoresistance (AMR)—the resistivity extrapolated back to zero

internal field ($B = 0$) depends on $\mathbf{M} \cdot \mathbf{J}$. The second effect is due to the ordinary (Lorentz) magnetoresistance and also in general anisotropic (*i.e.* dependent on $\mathbf{J} \cdot \mathbf{B}$). As Fe has a large magnetization and hence a large internal magnetic field ($4\pi M = 2.2$ T) both factors are of importance. The resistivity of domains parallel and perpendicular to the current direction can be written as:

$$\rho_{\perp}(B, T) = \rho_{\perp}(0, T)[1 + F_{\perp}(B/\rho_{\perp}(0, T))] \quad (1)$$

$$\rho_{\parallel}(B, T) = \rho_{\parallel}(0, T)[1 + F_{\parallel}(B/\rho_{\parallel}(0, T))] \quad (2)$$

here B is the internal field in the ferromagnet; $B = 4\pi M + H - H_d$, with H the applied field and H_d the demagnetization field. The AMR is proportional to $\rho_{\parallel}(0, T) - \rho_{\perp}(0, T)$. The function F is known as the Kohler function and parametrizes the ordinary magnetoresistance for longitudinal and transverse field geometry in terms of $B/\rho \sim \omega_c \tau$. With this form we have been able to determine the scaling functions F_{\perp} and F_{\parallel} [10] and $\rho_{\perp}(0, T)$ and $\rho_{\parallel}(0, T)$. At 40 K the AMR is $\sim 10^{-3}$. The fact that $\rho_{\perp}(H) > \rho_{\parallel}(H)$ in Fig. 4 (and thus that the resistivity anisotropy is opposite in sign to the AMR in this range of B fields) is a consequence of the ordinary MR (*i.e.* $F'_{\perp} > F'_{\parallel}$) [8].

The low field MR has been analyzed as follows. As this resistivity anisotropy is small and the domain size much greater than the mean free path we can write the effective resistivity in the $H = 0$ magnetic state as [11]:

$$\rho_{eff}(H = 0, T) = \gamma \rho_{\parallel}(B_i, T) + (1 - \gamma) \rho_{\perp}(B_i, T) \quad (3)$$

where γ is the volume fraction of domains oriented longitudinally and B_i is the field internal to these domains ($= 4\pi M - H_d$). We determine $\rho_{\perp}(B_i, T)$ and $\rho_{\parallel}(B_i, T)$ by extrapolation of the MR data above saturation (as indicated by the dashed lines in Fig. 4). With this model we estimate the low field MR associated with domain rotation and the sources of resistivity anisotropy discussed above. In the longitudinal geometry, at $H = 0$ the $1.5 \mu\text{m}$ wire consists predominately of domains perpendicular to \mathbf{J} ($\gamma = 0.18$). Thus ρ_{eff} is seen to be larger than that measured (see Fig. 4b). In the transverse case the measured resistivity is close to the

estimation of ρ_{eff} . In the transverse case the domain wall density is also 4 times smaller. For the 20 μm sample in both orientations the MR is consistent with estimations.

The deviations from this model $\rho_d = \rho(H = 0) - \rho_{eff}(H = 0)$, i.e., the measured $H=0$ resistivity minus the effective resistivity, are negative and depend systematically on domain wall density, increasing in magnitude with increasing domain wall density [8]. We also find that $|\rho_d|$ decreases with increasing temperature approaching zero at ~ 80 K (Fig. 5) and above. These deviations appear consistent with an enhancement of the conductivity associated with domain walls in these wires at low temperatures. In contrast to reports on Co and Ni films [1] [2], increasing resistivity due to domain walls at room temperature is not observed within the experimental uncertainty of $\rho_d/\rho(H = 0) \sim 10^{-3}$.

In summary, we have established a means of realizing magnetic microstructures with controlled domain patterns enabling new experimental studies of the role of domain boundaries on transport. The Lorentz MR is found to be important in determining the resistivity anisotropy and magnetotransport properties in these Fe wires. Our initial results also suggest that the presence of domain boundaries enhances the sample conductance. While an enhancement is consistent with a recent theory based on weak localization, the magnitude of the effect appears larger than predicted [5] and the effect is present up to ~ 80 K. These magnetic microstructures will certainly permit more detailed investigations of these novel effects.

ACKNOWLEDGEMENT

This research is supported by DARPA-ONR Grant# N00014-96-1-1207. Y. Z. is supported by AFOSR Grant# F49620-92-J-0190. We thank C. Noyan for x-ray characterization, H. Zhang and B. Sinkovic for help with MOKE, M. P. Sarachik for SQUID measurements and M. Ofitserov for technical assistance. Microstructures were prepared at the CNF, project #588-96.

REFERENCES

- [1] J. F. Gregg, et. al., “Giant magnetoresistance effects in a single element magnetic thin film,” *Phys. Rev. Lett.*, vol. 77, pp. 1580-1583, August 1996.
- [2] M. Viret, et. al., “Spin scattering in ferromagnetic thin films,” *Phys. Rev B*, vol. 53, pp. 8464-8468, April 1996.
- [3] P. M. Levy and S. Zhang, “Resistivity due to domain wall scattering,” *Phys. Rev. Lett.*, vol. 79, pp. 5110-5113, Dec. 1997.
- [4] K. Hong and N. Giordano, “Approach to mesoscopic magnetic measurements,” *Phys. Rev. B*, vol. 51, pp. 9855-9862, April 1995 and K. Hong and N. Giordano, preprint 1997.
- [5] G. Tatara and H. Fukuyama, “Resistivity due to a domain wall in ferromagnetic metal,” *Phys. Rev. Lett.*, vol. 78, pp. 3773-3776, May 1997.
- [6] B. M. Clemens, et. al., “In-situ observation of anisotropic strain relaxation in epitaxial Fe (110) films on Mo (110),” *J. of Mag. and Mag. Mat.*, vol. 121, pp. 37-41 Jan 1993.
- [7] In the case of a $0.65 \mu\text{m}$ wire there were noticeable differences in MR after this temperature and field cycling.
- [8] U. Ruediger, J. Yu, S. Zhang, A. D. Kent, and S. S. P. Parkin, “Negative domain wall contribution to the resistivity of microfabricated Fe wires,” to be published (1998).
- [9] see, for example, I. A. Campbell and A. Fert, ”Transport Properties of Ferromagnets,” in *Ferromagnetic Materials vol. 3*, E. P. Wohlfarth, Ed., North-Holland Pub. Co. 1982, pp. 747-806.
- [10] F. C. Schwerer and J. Silcox, “Electrical resistivity of Nickel at low temperatures,” *Phys. Rev. Lett.*, vol. 20, pp. 101-103, January 1968.
- [11] Since the current density in each domain is to a good approximation independent of the domain configuration this weighted average is appropriate.

FIGURES

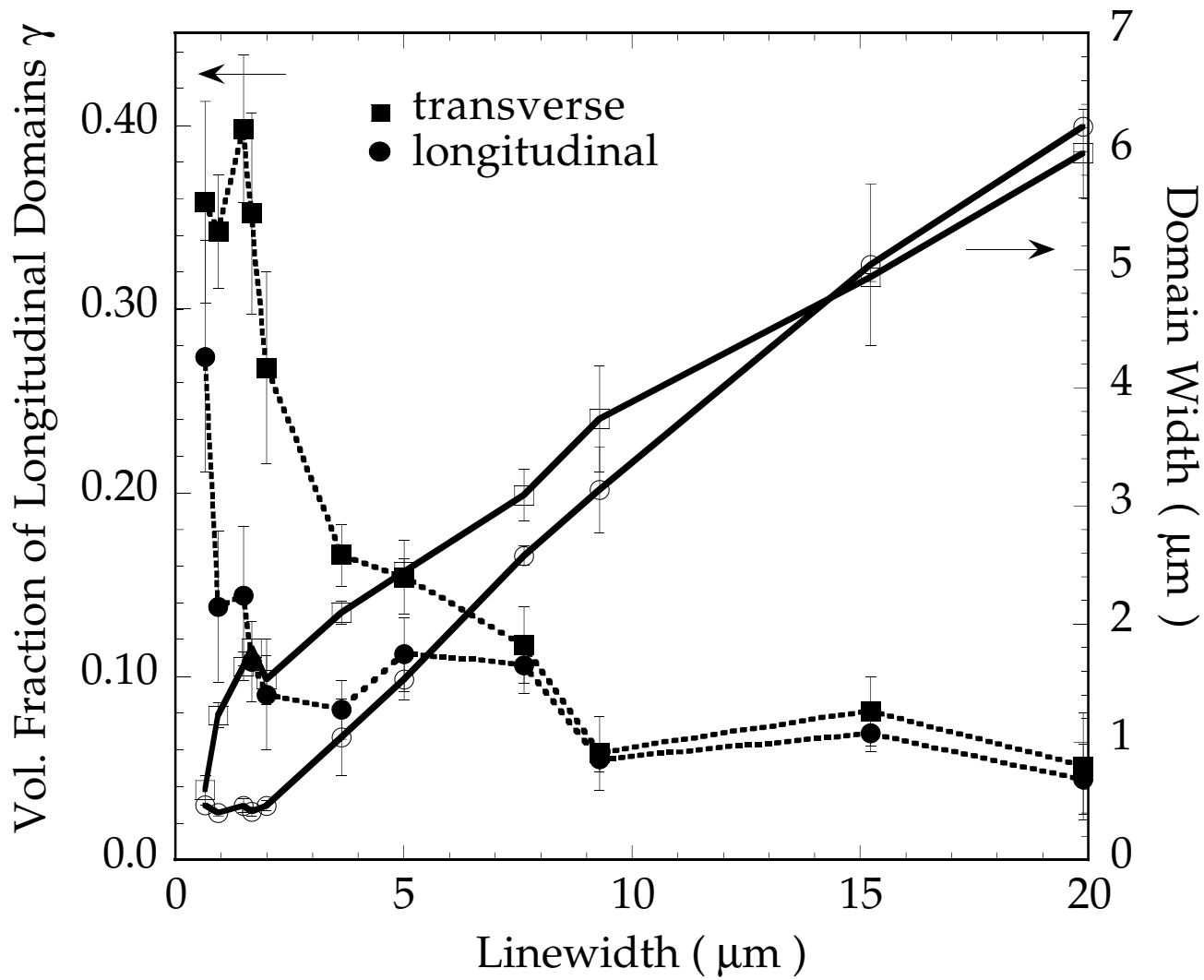
FIG. 1. Optical micrograph of 1 μm transport structure showing the Fe crystallographic orientation.

FIG. 2. MFM domain images in zero applied field for a) and b) a 1.5 μm and c) and d) a 20 μm linewidth wire. In a) and c) the wire is first magnetized transverse to the wire axis. In b) and d) the wire is first saturated along the wire axis.

FIG. 3. Heavy solid curve right hand axis: domain size along the wire axis after either transverse (solid squares) or longitudinal (solid circles) saturation versus linewidth. Volume fraction of longitudinally oriented closure domains after transverse (open squares) and longitudinal (open circles) saturation versus linewidth.

FIG. 4. MR data at 40 K of a 1.5 μm wire in a) a transverse and b) a longitudinal geometry $\rho_{\perp}(\text{H}=0, 40 \text{ K})=1.2 \mu\Omega\text{cm}$. Results from a 20 μm wire are shown in parts c) and d) $\rho_{\perp}(\text{H}=0, 40 \text{ K})=0.24 \mu\Omega\text{cm}$.

FIG. 5. ρ_d as a function of temperature for a 1.5 μm transport line.



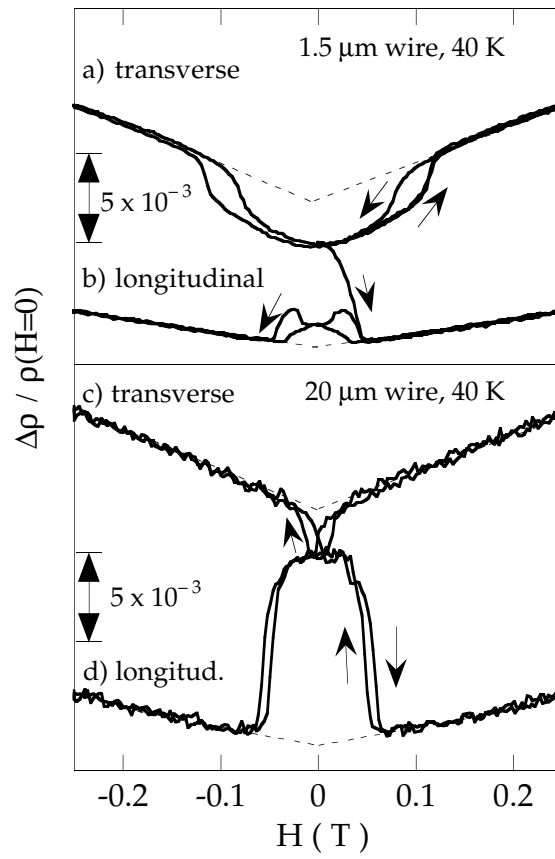


Fig.4, A. Kent

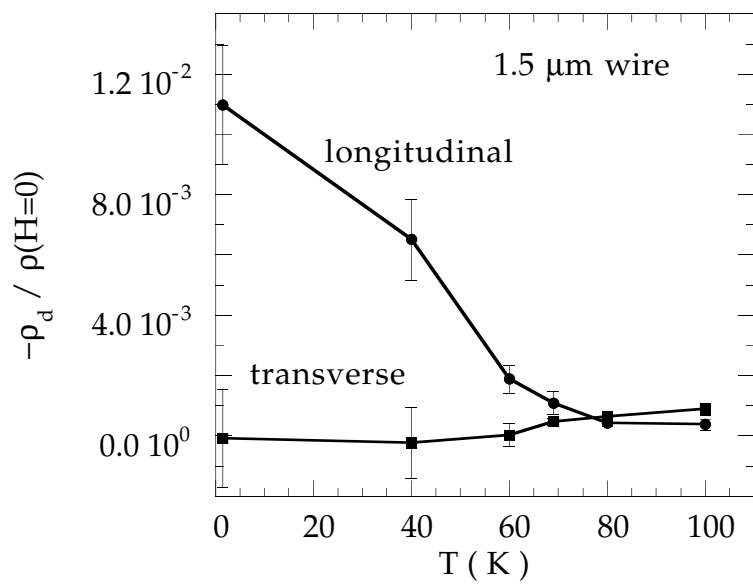


Fig.5, A. Kent

This figure "Fig1mag98.jpg" is available in "jpg" format from:

<http://arxiv.org/ps/cond-mat/9803101v1>

This figure "Fig2mag98.jpg" is available in "jpg" format from:

<http://arxiv.org/ps/cond-mat/9803101v1>